

# Boost in deep-UV electroluminescence from tunnel-Injection GaN/AlN quantum dot LEDs by polarization-induced doping

Jai K. Verma\*, Vladimir V. Protasenko, S. M. Islam, Huili Xing, Debdeep Jena  
Dept. of Electrical Engineering, Univ of Notre Dame, Notre Dame, IN USA 46556

\*jverma@nd.edu; phone 1 574 631-1290; fax 1 574 631-4393

## ABSTRACT

GaN/AlN quantum dots (QDs) have been observed to emit in deep ultra violet (UV) regime. The emission wavelength can be tuned from 270 nm to 238 nm using GaN growth time and Ga flux. In this work, tunnel injection GaN/AlN QD UV LEDs have been fabricated utilizing polarization doped p-n junctions grown on AlN templates on sapphire. The QD EL emission is obtained at 250 nm whereas a second peak emission is observed at 290 nm from the p-type AlGa<sub>N</sub>. However, the enhanced doping and carrier injection in polarization doped structure boosts the deep-UV emission intensity by 26 times compared to non-polarization doped UV LED.

**Keywords:** Quantum dot, Tunneling, UV LED, Polarization

## 1. INTRODUCTION

Light weight and robust ultraviolet (UV) light emitting sources find multitude of uses, for example in water purification, sterilization, bio sensors, solid state lighting and lithography. Direct bandgap III-Nitride semiconductors exhibit bandgap energies extending upto 6.2 eV (210 nm, deep UV). Thus, III-Nitrides are potential candidates for fabricating UV light emitting diodes (LEDs). But as we move to higher Al compositions to reach shorter wavelengths the internal quantum efficiency (IQE) severely degrades due to factors such as the valence band asymmetry, high threading dislocation densities, quantum confined Stark effect (QCSE) and inefficient n- and p-type doping.

### 1.1 GaN Quantum Dots

Quantum dots (QDs) are 0 dimensional nanostructures that provide 3D confinement of carriers leading to improved radiative recombination efficiency. This enables low threshold LEDs and lasers. III-Nitride (InAlGa<sub>N</sub>) QDs, grown by Stranski-Krastanov (SK) and anti-surfactant methods, have been shown to emit in the ultra violet (UV)<sup>1</sup> as well as in the visible spectral windows<sup>2</sup>. Due to strong carrier confinement, QDs favor significant increase in emission energy with decrease in the size of the dots for relatively low Al contents than in quantum wells. Tanaka *et al* had first achieved 3.55 eV emission from 6 nm thick and 40 nm wide GaN QDs embedded in AlGa<sub>N</sub> barriers grown by MOCVD through the anti-surfactant technique<sup>3</sup> and even stimulated emission at 3.49 eV<sup>4</sup>. Such GaN QDs were incorporated in LED structure to obtain electroluminescence (EL) at 360 nm<sup>5</sup>. The large lattice mismatch (2.4 %) between GaN and AlN is conducive to island formation. At substrate temperatures higher than 700°C, SK growth mode was found to be active in formation of self assembled GaN QDs on AlN substrate in N-rich growth regime by molecular beam epitaxy (MBE)<sup>6</sup>.

262 nm (~ 4.7 eV) emission has been obtained from the 2 monolayer (ML) thick wetting layer of the GaN QDs<sup>7</sup>. Brown *et al* also observed high energy emission at 4.7 eV and 5.1 eV from the quantum well (QW) formed by the GaN wetting layer<sup>8</sup>. The blue emission generally obtained from thick GaN QDs is attributed to the QCSE. As the QD height was reduced from 5 ML to 3 ML, the emission wavelength shifted from 440 nm to 310 nm<sup>9</sup>. Kamiya *et al* have calculated that GaN/AlN superlattice structures are very well capable to achieve deep-UV emission (< 300 nm)<sup>10</sup>. The shortest wavelength was calculated to be 224 nm from 1 ML thick GaN layer. Thus, it is feasible to produce deep-UV emission from ultra-small GaN/AlN structures. EL has been obtained using GaN/AlN active region spanning the wavelength region from 275.8 nm to 236.9 nm<sup>11</sup>. Recently, we demonstrated a different approach incorporating 2 monolayer (ML) thick GaN quantum dots (QDs) to obtain EL at 261 nm through tunnel injection and transport of carriers<sup>12</sup>. In our design, the spatial distribution of electron and hole wavefunctions in pyramidal GaN QDs<sup>13</sup> as well as the thin AlN barrier promotes tunneling transport of carriers (electrons and holes) despite the large effective mass of holes. This is because quantum confinement shifts the eigenvalues to higher energies, which in turn extends deep into the barriers. Since tunneling is the mode of transport, we need n- and p- type contact regions that absorb just above the emission wavelength of the QDs, leading to a relatively low composition AlGa<sub>N</sub> layers resulting in improved doping. Besides, the much speculated phonon bottleneck<sup>14</sup> problem associated with QD systems can be overcome, as the carriers are

injected directly into the lowest energy state of the dots. Therefore, as a consequence, QDs in the active region can offer solutions to most of the issues plaguing high Al content in UV LEDs.

## 1.2 Polarization-induced doping

Obtaining high hole concentrations in III-nitrides is difficult due to large activation energy  $E_A$ : 200 meV<sup>15</sup> of Mg in GaN. The situation becomes worse in high Al composition AlGaN alloys, since the Mg activation energy in AlN is even higher ( $E_A$ : 630 meV)<sup>15</sup>. Low hole concentrations combined with low hole mobilities make the p-side of LEDs highly resistive, causing high losses. In UV LEDs fabricated using AlGaN alloys, it has remained difficult to fabricate low-resistance ohmic contacts to p-AlGaN because of the low hole concentration. To lower the ohmic contact resistance, usually a p-GaN cap layer is used, but this layer absorbs a portion of the UV light emitted in the active region, leading to reduced extraction efficiency of LED. In compositionally graded heterojunctions along  $\langle 0001 \rangle$  the polarization-induced sheet charge is spread into a 3D bound charge given by  $\rho_\pi = -\nabla \cdot (P_1 - P_2)$  C/cm<sup>3</sup><sup>16</sup>. This fixed bulk polarization charge attracts oppositely charged mobile carriers to satisfy local charge neutrality. The creation of mobile charges is tantamount to doping. Jena *et al* demonstrated n-type doping by compositionally grading AlGaN along the metal face<sup>17</sup>. Since the polarization-induced doping process is purely electrostatic, it has no thermal activation energy, and the mobile carriers do not freeze out at low temperatures. p-type polarization induced doping has also been demonstrated to improve light emission in UV LEDs<sup>15</sup>. Following this demonstration p-type doping for metal face crystal orientation was obtained by downgrading 30% AlGaN to GaN<sup>18</sup>. In this work we have utilized similar downgrading of AlGaN composition to improve the emission intensity of tunnel injection GaN/AlN QD UV LEDs grown by plasma assisted MBE (PAMBE).

## 2. EXPERIMENTAL WORK

### 2.1 MBE growth and Fabrication of UV LEDs

The growth of GaN/AlN QD UV LED structures is performed by PAMBE. The N<sub>2</sub> flow rate is maintained at 1.2 sccm resulting in a growth chamber pressure of  $2 \times 10^{-5}$  Torr. 225 W RF plasma power is utilized for a growth rate of 0.173 ML/s in the growth of all the structures. The AlN nucleation and buffer layers are grown under III/N~1 conditions at a substrate temperature of  $T_c \sim 730^\circ\text{C}$  and an Al flux of  $6.7 \times 10^{-8}$  Torr to obtain very smooth surface morphology. The stoichiometric conditions are found by observing the RHEED pattern for the streak formed by excess Al<sup>19</sup> as shown in Figure 1. In our earlier report we had observed bimodal distribution driven double-peak emission from the dots grown in SK mode<sup>12</sup>. By successively reducing the GaN dot growth time from 35 to 25 sec, we found that the RT optical emission blue shifts from 270 nm  $\rightarrow$  246 nm as seen in the photoluminescence spectra<sup>20</sup>. At the same time, the emission becomes single-peaked, showing a reduction in the bimodal size distribution, and in particular the  $\sim 340$  nm peak. Further by reducing the Ga flux from  $6.2 \times 10^{-8}$  Torr to  $5.6 \times 10^{-8}$  Torr while keeping the dot growth time constant at 25 sec, the emission peak could be further blue-shifted to 238 nm.

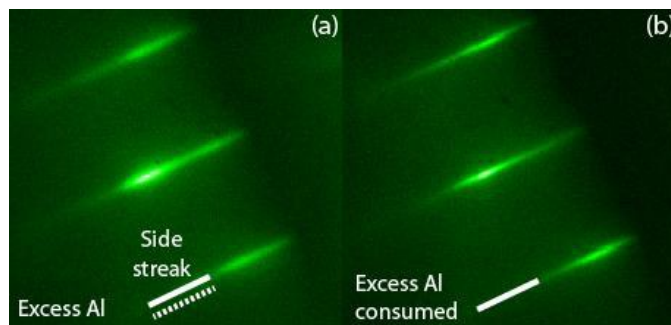


Figure 1. (a) RHEED pattern shows 1st order streaks from excess Al overlayer when viewed along  $[11-20]$  for Al-rich growth (b) RHEED pattern shows bright sharp streaks when excess Al gets consumed.

The active region of the two LEDs consists of 8-periods of the GaN quantum dot/AlN barrier heterostructure as shown in Figure 2(a). The active region quantum dots were grown in the Stranski-Krastonov mode with 25 s growth time. The n-injection layer for all three LEDs is a  $\sim 225$  nm Si-doped high composition AlGaN with doping density  $N_D \sim 5 \times 10^{19}/\text{cm}^3$ . The p-injection region for the three LEDs is varied to demonstrate the effect of light reabsorption and polarization-induced doping. The layer composition details are highlighted in the measured X-ray diffraction patterns. Sample I has a uniform Mg-doped  $\text{Al}_{0.5}\text{Ga}_{0.5}\text{N}$  as the p-contact layer, and serves as the control sample. Samples II

incorporates compositionally graded  $\text{Al}_x\text{Ga}_{1-x}\text{N}$  p-type layer. The linear grading is from  $x = 0.51 \rightarrow 0.27$  for Sample II which is achieved by varying the Al metal flux during the MBE growth; because the flux depends exponentially on the effusion cell temperature  $F_{\text{Al}} \propto \exp(-E_{\text{Al}}/k_{\text{B}}T_{\text{Al}})$  with an activation energy  $E_{\text{Al}}$ , the cell temperature  $T_{\text{Al}}$  is changed accordingly with time. The thickness of the p-layers was  $\sim 117$  nm for both the samples, and the Mg doping was  $N_{\text{A}} \sim 4 \times 10^{19}/\text{cm}^3$ . The expected polarization induced doping is  $\rho_{\pi} = -\nabla \cdot \mathbf{P} \sim 1 \times 10^{18}/\text{cm}^3$ . Figure 2(b) shows the schematic band diagram for Samples I and II along with the tunneling and recombination mechanisms. A p-n junction control sample was also grown with 50% AlGaN composition. After epitaxial growth, LEDs were fabricated by etching 200 nm deep mesas, and depositing Ti/Al/Ni/Au (20/100/40/50 nm) metal stacks on the etched n-AlGaN surface for n-type contacts, and thin Ni/Au (5/5 nm) thin transparent p-type current spreading layer on the mesa surface. Thicker Ti/Au (20/100 nm) probe pads were deposited on the p-contacts as shown in Figure 2(a). The LEDs that were studied for electroluminescence were  $150 \times 450 \mu\text{m}^2$  in size.

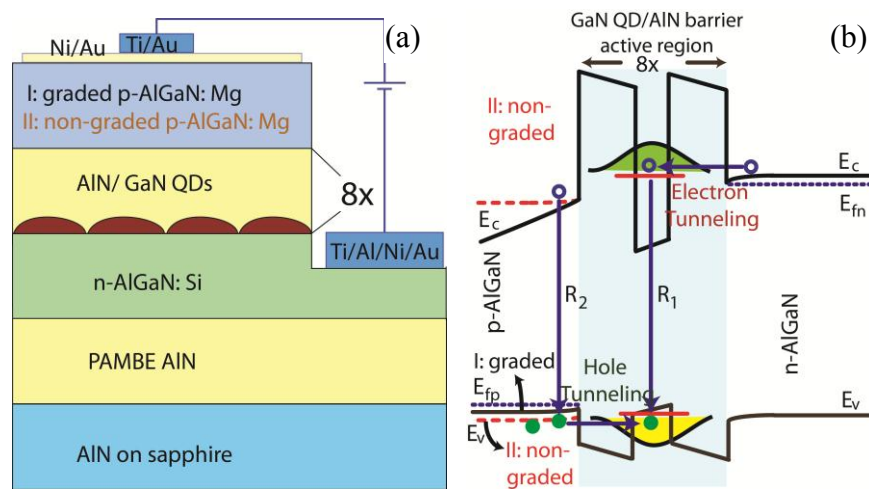


Figure 2. (a) Schematic sketch of the UV LED structure with metal contacts (b) Schematic band diagram for Sample I and II showing the tunneling mechanism and recombination in QDs and p-AlGaN layer.

### 3. RESULTS AND DISCUSSION

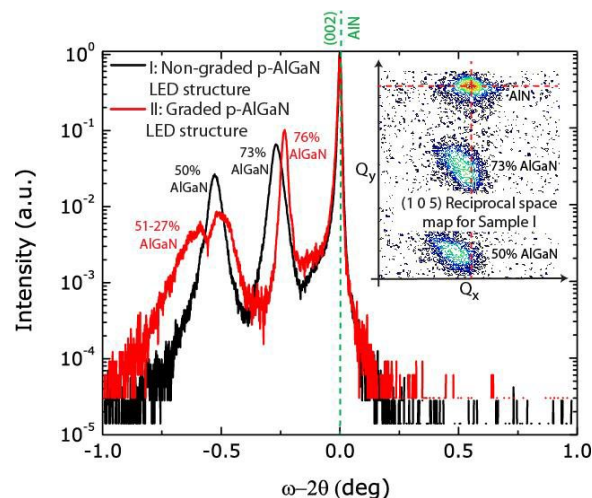


Figure 3. Triple-axis  $\omega$ - $2\theta$  scans show the difference between graded and non-graded AlGaN layers. Inset: (105) reciprocal space map of Sample I shows that the AlGaN layers are not completely relaxed with respect to AlN.

Triple axis  $\omega$ - $2\theta$  scans were conducted on Samples I and II as shown in Figure 3. Sample II shows the effect of grading in the AlGaN layer. Fitting the measured data with simulation provides us with the layer compositions which are shown

in Figure 3. Reciprocal space map study of Sample I for (105) orientation (Figure 3: Inset) shows strained growth of AlGaIn layers with respect to AlN.

The processed LED structures were subjected to electrical measurements. The EL spectrum from the control AlGaIn p-n junction shows weak emission around 295 nm at very high injection current densities (Figure 4(a)). Sample I shows prominent 290 nm emission which is attributed to recombination ( $R_2$ ) occurring in the p-AlGaIn layer due to leakage of electrons as well as excitation of p-AlGaIn layer by the light emitted from the QDs (Figure 4(b)). The EL emission intensity is found to increase with injection current density. Besides, due to the low hole concentration in sample I, the hole injection into QDs is poor resulting in weak emission from QDs.

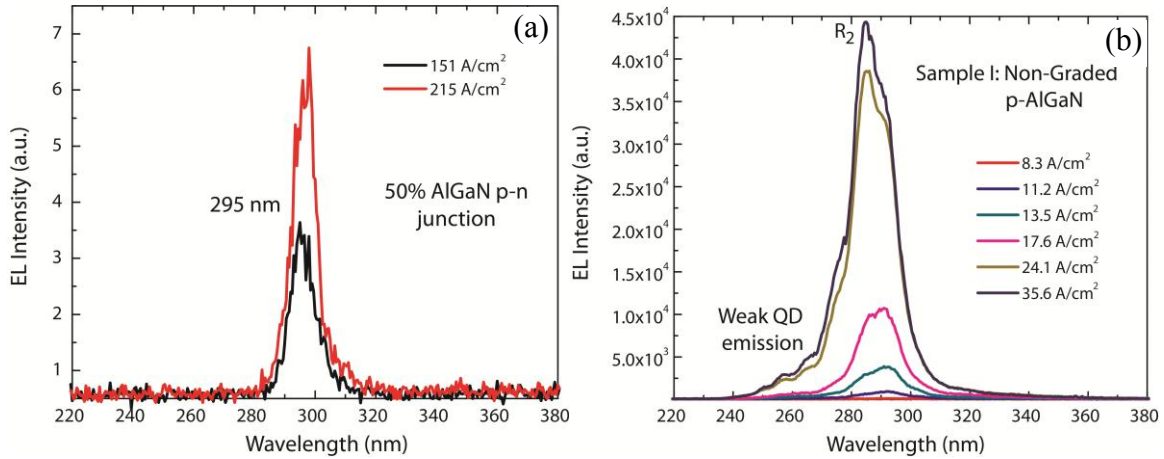


Figure 4. (a) EL spectra from 50% AlGaIn p-n junction shows very weak emission at 295 nm at high current densities (b) EL spectra from Sample I shows increasing emission intensity with injection current density. The main emission peak is from p-AlGaIn layer and the QD emission is observed to be weak.

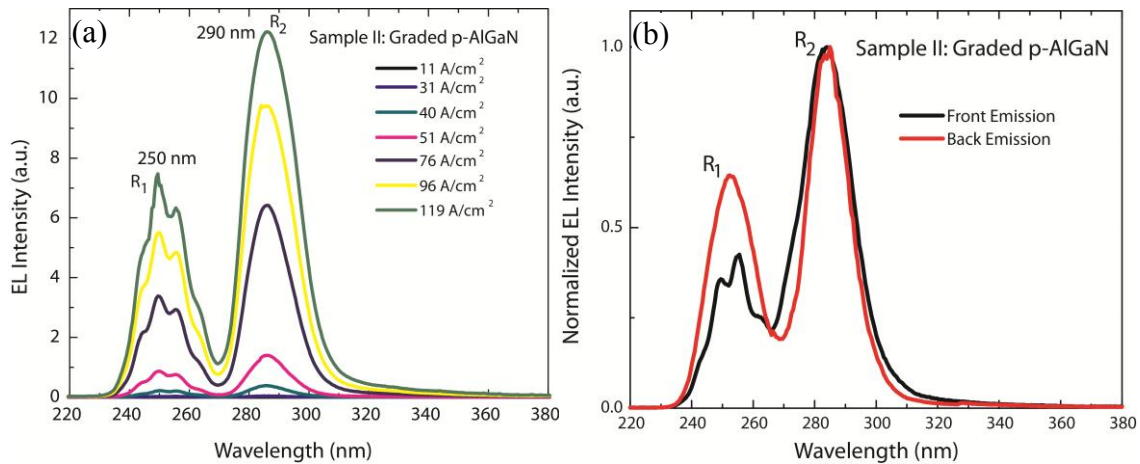


Figure 5. (a) EL spectra from Sample II shows increasing emission intensity with injection current density with double peaks. The 290 nm emission is attributed to p-AlGaIn layer and the 250 nm emission is from QD quantized energy levels. (b) A comparison of EL spectra collected from the top and back side shows that the ratio between the peaks from QD and p-AlGaIn is higher for back side collection. This signifies absorption of photons, emitted from the QDs, in the p-AlGaIn layer.

Figure 5(a) shows the EL spectra taken from Sample II. As a result of an enhanced hole density, the net EL emission intensity is significantly enhanced compared to the control sample, as will be discussed shortly. The EL spectra show a strong  $R_1$  peak at 250 nm in addition to the same  $R_2$  peak as sample I. In spite of the polarization induced doping boost in hole concentration, significant electron leakage into this layer, and reabsorption of  $R_1$  photons both result in a strong  $R_2$  peak. Figure 5(b) shows a comparison of the EL spectrum collected from the back side and top side of the LED from sample II. The ratio of  $R_1$  to  $R_2$  emission is higher for back side collection signifying that the emission from QDs is absorbed to some extent in the top p-AlGaIn layer. In Figure 6, the EL spectra of samples I and II are compared.

Polarization-included p-type doping boosts the integrated EL emission intensity from sample II by 26× compared to sample I at an injection current level of  $J_{inj} \sim 24 \text{ A/cm}^2$ .

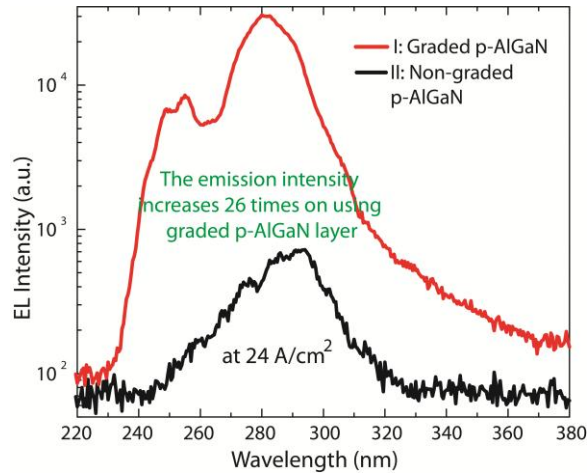


Figure 6. EL spectra from Sample II is 26 times than from Sample I as a result of improved hole concentration due to polarization induced doping.

Figure 7 shows the measured current voltage characteristics of the control p-n junction sample along with samples I and II. The IV curves show weak rectification for samples I and II whereas for the control sample the IV curves are very symmetrical about 0V.

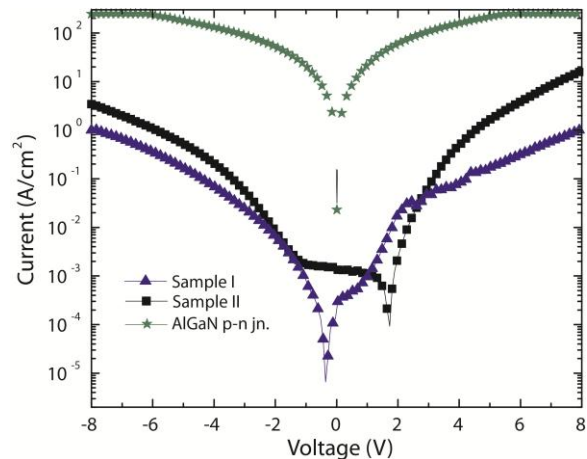


Figure 7. IV curves from control AlGaIn p-n junction, sample I and II. Weak rectification is observed.

#### 4. CONCLUSION

In summary, we demonstrate that 250 nm deep-UV emission can be obtained from GaN quantum dots in the extreme quantum-confinement limit at room temperature by electrical injection. The GaN active region comprising of ultrasmall GaN dots embedded in an AlN matrix enables tunnel-injection of carriers from the n- and p-injection regions. Quantum confinement prevents lateral diffusion of carriers to non-radiative recombination sites, and tunnel-injection enables a balanced injection of electrons and holes. The design also incorporates polarization-induced doping for improving p-type doping. The emission from p-AlGaIn can be removed by using a further high composition graded p-AlGaIn layer<sup>20</sup>. The demonstration thus paves the way to improved radiative recombination, lower heat generation, improved light extraction, and more efficient doping, all of which remain major roadblocks to improving the efficiency of deep-UV LEDs.

## REFERENCES

- [1] Hirayama, H. and Fujikawa, S., "Quaternary InAlGa<sub>n</sub> quantum-dot ultraviolet light-emitting diode emitting at 335 nm fabricated by anti-surfactant method," *Phys. Stat. Sol. (c)* 5(6), 2312-2315 (2008).
- [2] Moustakas, T. D., Xu, T., Thomidis, C., Nikiforov, A.Y., Zhou, L., and Smith, D.J., "Growth of III-nitride quantum dots and their applications to blue-green LEDs," *Phys. Stat. Sol. (a)* 205(11), 2560–2565 (2008).
- [3] Tanaka, S., Iwai, S. and Aoyagi, Y., "Self assembling GaN quantum dots on Al<sub>x</sub>Ga<sub>1-x</sub>N surfaces using a surfactant," *Appl. Phys. Lett.* 69, 4096 (1996).
- [4] Tanaka, S., Hirayama, H., Aoyagi, Y., Narukawa, Y., Kawakami, Y., Fujita, S. and Fujita, S., "Stimulated emission from optically pumped GaN quantum dots," *Appl. Phys. Lett.* 71, 1299 (1997).
- [5] Tanaka, S., Lee, J.-S., Tamvall, P. and Okagawa, H., "A UV Light-Emitting Diode Incorporating GaN Quantum Dots," *Jpn. J. Appl. Phys.* 42, L885–L887 (2003).
- [6] Daudin, B., Widmann, F., Feuillet, G., Samson, Y., Arlery, M. and Rouvie`re, J. L., "Stranski-Krastanov growth mode during the molecular beam epitaxy of highly strained GaN," *Phy. Rev. B*, 56( 12), R7069-R7072 (1997).
- [7] Miyamura, M., Tachibana, K. and Arakawa, Y., "UV Photoluminescence from Size-Controlled GaN Quantum Dots Grown by MOCVD," *Phys. Stat. Sol. (a)* 192(1), 33–38 (2002).
- [8] Brown, J. S., Petroff, P. M., Wu, F. and Speck, J. S., "Optical Properties of GaN/AlN(0001) Quantum Dots Grown by Plasma-Assisted Molecular Beam Epitaxy," *Jpn. J. Appl. Phys.*, 45, L669 (2006).
- [9] Renard, J., Kandaswamy, P. K., Monroy, E. and Gayral, B., "Suppression of nonradiative processes in long-lived polar GaN/AlN quantum dots," *Appl. Phys. Lett.* 95, 131903 (2009).
- [10] Kamiya, K., Ebihara, Y., Shiraishi, K. and Kasu, M., "Structural design of AlN/GaN superlattices for deep-ultraviolet light-emitting diodes with high emission efficiency," *Appl. Phys. Lett.* 99, 151108 (2011).
- [11] Taniyasu, Y. and Kasu, M., "Polarization property of deep-ultraviolet light emission from C-plane AlN/GaN short-period superlattices," *Applied Physics Letters* 99, 251112 (2011).
- [12] Verma, J., Kandaswamy, P. K., Protasenko, V., Verma, A., Xing, H. and Jena, D., "Tunnel-injection GaN quantum dot ultraviolet light-emitting diodes," *Applied Physics Letters* 102, 041103 (2013).
- [13] Andreev, A. D. and O'Reilly, E. P. "Theory of the electronic structure of GaN/AlN hexagonal quantum dots," *Phy. Rev. B* 62(23), 15851-15870 (2000).
- [14] Sugawara, M., Mukai, K. and Shoji, H., "Effect of phonon bottleneck on quantum-dot laser performance," *Appl. Phys. Lett.* 71, 2791 (1997).
- [15] Simon, J., Protasenko, V., Lian, C., Xing, H. and Jena, D., "Polarization-Induced Hole Doping in Wide-Band-Gap Uniaxial Semiconductor Heterostructures," *Science*, 327, 60-64 (2010).
- [16] Jena, D., "Polarization induced electron populations in III-V nitride semiconductors: Transport, growth and device applications," PhD thesis UCSB (2003).
- [17] Jena, D., Heikman, S., Green, D., Buttari, D. and Coffie, R., "Realization of wide electron slabs by polarization bulk doping in graded III-V nitride semiconductor alloys," *Applied Physics Letters* 81, 4395-4397 (2002).
- [18] Zhang, L., Ding, K., Yan, J. C., Wang, J. X., Zeng, Y. P., Wei, T. B., Li, Y. Y., Sun, B. J., Duan, R. F. and Li, J. M. "Three-dimensional hole gas induced by polarization in (0001)-oriented metal-face III-nitride structure," *Applied Physics Letters* 97, 062103 (2010).
- [19] Lee, C. D., Donga, Y., Feenstra, R. M., Northrup, J. E. and Neugebauer, J., "Growth and Surface Reconstructions of AlN(0001) Films," *Materials Research Society Symposium Proceedings* 798, Y.3.5.1 (2004).
- [20] Verma, J., Islam, S.M., Protasenko, V., Kandaswamy, P. K., Xing, H. and Jena, D., "Tunnel-Injection Quantum Dot deep-Ultraviolet Light-Emitting Diodes with Polarization-Induced Doping in III-Nitride Heterostructures," *Applied Physics Letters* (accepted for publication) (2014).